*Original Research*

# Ligand exchange on gold nanoparticles for drug delivery and enhanced therapeutic index evaluated in acute myeloid leukemia models

**Shunji Egusa[1], Quteba Ebrahem[1], Reda Z Mahfouz[1] and Yogen Saunthararajah[1,2]**

[1]Department of Translational Hematology and Oncology Research, Taussig Cancer Institute, The Cleveland Clinic Foundation, Cleveland, Ohio 44195, USA; [2]Department of Hematologic Oncology and Blood Disorders, Taussig Cancer Institute, The Cleveland Clinic Foundation, Cleveland, Ohio 44195, USA

Corresponding author: Yogen Saunthararajah. Email: saunthy@ccf.org

## Abstract

Cancer chemotherapy is typically toxic. This problem could be addressed by using differences between cancer and normal cells for controlled delivery of drugs to cancer cells. One such difference is the ubiquitously elevated glutathione expression in cancer cells. We report a simple and versatile synthesis of water-soluble gold nanoparticles passivated with amine-containing molecules, which allow for controlled drug release via ligand exchange with bio-available glutathione. Taking methotrexate-passivated gold nanoparticles (Au:MTX) as an example, drug delivery and controlled release via glutathione-mediated ligand exchange was evaluated. Furthermore, the possibility of using Au:MTX to improve therapeutic index in acute myeloid leukemia (AML) models was examined *in vitro* and *in vivo*. Au:MTX exhibited cancer selectivity *in vitro*. Au:MTX had an elevated potency toward an AML cell line THP-1 in a dosage range of 1–5 nM, and therefore an enhanced delivery of drug, whereas normal hematopoietic stem/progenitor cell (HSPC) growth was minimally affected by Au:MTX and MTX treatments within the same range of dosage. *In vivo* efficacy and safety of Au:MTX was evaluated in a murine xenotransplant model of primary human AML. Au:MTX treatment, compared to control groups including MTX-only and Au nanoparticle-only treatments, produced better leukemia suppression without added toxicity, indicating an enhanced therapeutic index.

**Keywords:** Nanoparticles, drug delivery, amine, methotrexate, leukemia, cancer

***Experimental Biology and Medicine* 2014; 239: 853–861. DOI: 10.1177/1535370214536648**

## Introduction

An enduring, fundamental issue in cancer medicine is that of poor therapeutic index: treatments typically destroy normal as well as cancer cells, causing substantial toxicity that limits the safety and efficacy of treatment.[1] Thus there is a need for methods to more selectively deliver drugs to cancer cells and thereby spare normal cells.[2–4] Au nanoparticles, along with other drug delivery technologies such as micellar and liposomal[5–7] or polymeric encapsulations,[8–12] and monoclonal antibody conjugation,[13–15] have been intensively pursued as candidates to improve cancer therapeutics.[16–20] An important aspect of Au nanoparticles is that their physical properties as well as interactions with bio-organisms can be controlled by their size and shape,[21–23] and the careful engineering of these combined effects have culminated in various theranostic applications.[16–20] Au nanoparticles are typically passivated with thiol-containing molecules via strong thiol-to-Au bond,[24–26] and some of the delivery mechanisms by the thiol-passivated Au nanoparticles have been elucidated: these include (i) accumulation based on EPR (enhanced permeability and retention) effect[27] observed for relatively large-sized nanoparticles (~15–100 nm)[16–20] in solid tumor models, and (ii) various payload release mechanisms including, for example, pH change[28,29] or triggering by endogenous glutathione utilizing thiol-to-thiol ligand exchange.[30,31] Herein, glutathione-mediated ligand exchange[31,32] could be a promising scheme of controlled intracellular payload release *in vivo*, exploiting higher level of cell-associated glutathione compared to that of plasma.[33] Because ligand exchange is based upon competitive affinity to Au surface between the original and the incoming ligands,[30] a wider range of payload release kinetics would become available by exploiting Au nanoparticles directly passivated with payloads as ligands, through functional groups with weaker affinity to Au than that of thiols such as amines, carboxyls, phosphines, etc. (principle of ligand exchange, utilizing the differential in the affinity to Au, has been described by Hutchison *et al.*[34,35]). Passivation relying on weak Au affinity would seem at first to inhibit the

formation of Au nanoparticles, or to sacrifice the colloidal stability especially under physiologically relevant conditions. Here, we report the versatile synthesis of small (~2.5 nm) water-soluble Au nanoparticles that are directly passivated with amine-containing molecules. Taking methotrexate-passivated Au nanoparticles (Au:MTX) as an example, we examine the stability in physiological environments, and demonstrate the payload (*i.e.* MTX) release triggered by glutathione. Furthermore, we demonstrate improved therapeutic index *in vitro* using a cancer/normal cell comparison, and *in vivo* using a murine xenotransplant model of primary human acute myeloid leukemia (AML), a cancer which is disseminated without large tumor masses, and therefore in which there should be less benefit, if any, from EPR effect.[27]

## Materials and methods

### Materials

All chemicals were used as received (from Sigma-Aldrich, St. Louis, MO, USA) except otherwise noted, including water (HPLC grade, Honeywell Burdick & Jackson, Muskegon, MI, USA), methanol (ACS grade, Thermo Fisher Scientific, Pittsburgh, PA, USA), and ethanol (absolute, Pharmaco-Aaper, Brookfield, CT, USA).

### Au:MTX synthesis and characterization

In a typical synthesis of water-soluble nanoparticles, Au:MTX, 5 μmol of $HAuCl_4$, and 25 μmol of MTX were dispersed with brief sonication in 2 mL methanol in a tri-neck 15 mL flask on ice water (0°C) bath under Ar purge. After 1 h of stirring at 700 rpm, 0.5 mL of freshly prepared 0.11 M $NaBH_4$ on ice was added drop-wise at 1200 rpm. After ~1 h, stirring speed was reduced to 700 rpm and kept for additional ~30 min. Scale-up of the reaction has been confirmed up to 20-fold, yielding consistent results by transmission electron microscopy (TEM) characterization.

### Au:MTX nanoparticle purification and determination of drug loading

The reacted solution was centrifuged at 4°C at 16,100 × *g* for 15 min twice, with the addition of 4:1 (volume) mixture of methanol and water, and ethanol, respectively. This set of two-step centrifugation was repeated at least three times, and then the precipitate was redispersed in water to obtain aqueous solutions. The aqueous solution was further purified using 3 k ultra centrifugal filter (Millipore, Billerica, MA, USA). Following the sets of centrifugations of Au:MTX as described above, purity of Au:MTX was verified by sodium dodecyl sulfate polyacrylamide gel electrophoresis (SDS-PAGE). Elemental analytic measurements (Galbraith Laboratories, Inc., Knoxville, TN, USA) including carbon-hydrogen-nitrogen analysis (CHN) and inductively coupled plasma mass spectrometry (ICP-MS) confirmed the purity of the compound, where absence of organics other than MTX was verified via CHN, and Au-to-MTX ratio [Au]:[C]:[N] was determined via CHN and ICP-MS.

### Ligand exchange induced by glutathione and release of MTX from Au:MTX

Aqueous solution of Au:MTX (1 mM, in Au molar amount) was mixed with glutathione (GSH; 0.5, 1, or 5 mM) under 700 rpm stirring at room temperature, to induce MTX-to-GSH ligand exchange. Aliquot was diluted in water and extinction spectrum was measured using ultraviolet-visible (UV–vis) optical spectroscopy. The amount of released free MTX in solution was evaluated by extinction spectra at 90 minutes of stirring. The ligand exchange process was monitored up to 15 h.

### Evaluation of Au:MTX nanoparticle efficacy in vitro

In order to evaluate the efficacy of Au:MTX *in vitro*, we used a human AML cell line THP-1 and human normal hematopoietic stem/progenitor cells (HSPCs). HSPCs were isolated from umbilical cord blood via a CD34+ magnetic cell sorting (CD34 MicroBead Kit #130-046-702, Miltenyl Biotec, Auburn, CA, USA). THP-1 cells were cultured in Roswell Park Memorial Institute 1640 (RPMI, Life Technologies, Carlsbad, CA, USA) with 10% fetal bovine serum (FBS, Life Technologies), and HSPCs were cultured in Iscove's Modified Dulbecco's Medium (IMDM, Life Technologies) with 10% FBS and cytokines (10 ng/mL of SCF, TPO, and FLT3; 5 ng/mL of IL-3 and IL-6, PeproTech, Rockey Hill, NJ, USA), respectively, using 24-well cell culture plates with 0.7 mL of culture media per well (at 37°C with 5% $CO_2$ and >95% humidity). Cell viability was confirmed to be >95% using cell viability analyzer (Vi-Cell, Beckman Coulter, Brea, CA, USA) immediately before the experiments. Then the cells were treated with phosphate buffer saline (PBS, Life Technologies), MTX, aqueous solutions of equimolar Au:MTX, and/or equimolar Au:FOL (folic acid-passivated Au nanoparticles). Cell cultures were split two-fold after 72 h by replenishing each well with fresh media. Cell density and viability were measured every 24 h using the cell viability analyzer. For the evaluation of cellular uptake of Au:MTX, THP-1 cells were treated with 500 nM Au:MTX for 4 h via incubation at the culturing conditions, then the cells were centrifuged, and the resulting pellets were washed with PBS and dispersed in a standard TEM fixative (100 mM sodium cacodylate buffer with 4% paraformaldehyde and 2.5% glutaraldehyde), resin sectioned and mounted on nickel TEM grid. The specimens thus prepared were silver-enhanced (following the protocol associated with Silver Enhancer Kit #SE100, Sigma-Aldrich) and imaged by TEM.

### Au:MTX treatment on murine models and evaluation of tumor burden

The animal experiments were conducted with the approval of the Cleveland Clinic Foundation's Institutional Animal Care and Use Committees (IACUC). Primary AML cells were transplanted in 6-week old non-obese diabetic severe combined immunodeficiency gamma (NSG) mice by tail vein intravenous (i.v.) injection. Five days post-transplantation, treatments with Au:MTX, along with MTX (as drug-only control), Au:FOL (as nanoparticle-only control),

and PBS were initiated (five mice per group, total of 20 mice). Mice were treated by tail vein i.v. injection metronomically twice per week under daily surveillance. Aqueous solutions of Au:MTX and Au:FOL, as well as stock solution of MTX in dimethyl sulfoxide (0.1 μL per gram of mouse weight per treatment), were diluted with PBS for i.v. injections. Mice were sacrificed according to the IACUC-approved protocol, when the PBS-treated group showed clear signs of anemia and distress. Murine bone marrows were analyzed by flow cytometry (CYTOMICS FC 500, Beckman Coulter), where the populations of human AML cells and mouse hematopoietic cells were determined by staining with ECD-conjugated anti-human CD45 monoclonal antibody (mAb) and APC-conjugated anti-mouse CD45 mAb, respectively (Beckman Coulter). Spleens, livers, and intestines were harvested and fixed in 4% paraformaldehyde and embedded in a paraffin block. The tissues were sectioned (5 μm thick), hydrated via immersions in xylene (3 times) and ethanol (100%, 95%, and 75% successively), and then silver-enhanced and co-stained with hematoxylin and/or eosin.

### Glutathione assay of cancer and normal hematopoietic lineage cells

Viability of THP-1, primary AML cells, and normal HSPCs was confirmed to be >95% using a cell viability analyzer immediately before experiments. Intracellular glutathione concentration was measured using ~$10^7$ cultured cells (following the protocol associated with the Glutathione Assay Kit #CS0260, Sigma-Aldrich).

## Results

### Synthesis of Au nanoparticles passivated by amine-containing molecules

Compared to the extensive library of thiol-passivated nanomaterials,[24–26] there are fewer examples of amine-passivated nanoparticles,[36,37] particularly water-soluble amine-Au nanoparticles.[38–41] Using a simple variation of the method described by Schaaf *et al.* for synthesizing thiol-passivated ultra-small Au nanoparticles[42,43] and of the original method of Brust *et al.*,[44] we were able to synthesize water-soluble Au nanoparticles directly passivated with a monolayer of the chemotherapeutic methotrexate (Au:MTX) (Figure 1(a) to (c); 2.6 ± 0.7 nm in diameter, measured by transmission electron microscopy or TEM; also see Figure S1, Supplementary data available online), without necessitating post-synthesis chemistry.[45] Proton nuclear magnetic resonance ($^1$H NMR; Bruker, 600 MHz) measurements of Au:MTX in $D_2O$ indicated large change of chemical shift (in Figure 1(d), a: $\Delta\delta = 0.30$ ppm; b: $\Delta\delta = 0.23$ ppm; c: $\Delta\delta = 0.39$ ppm) in the

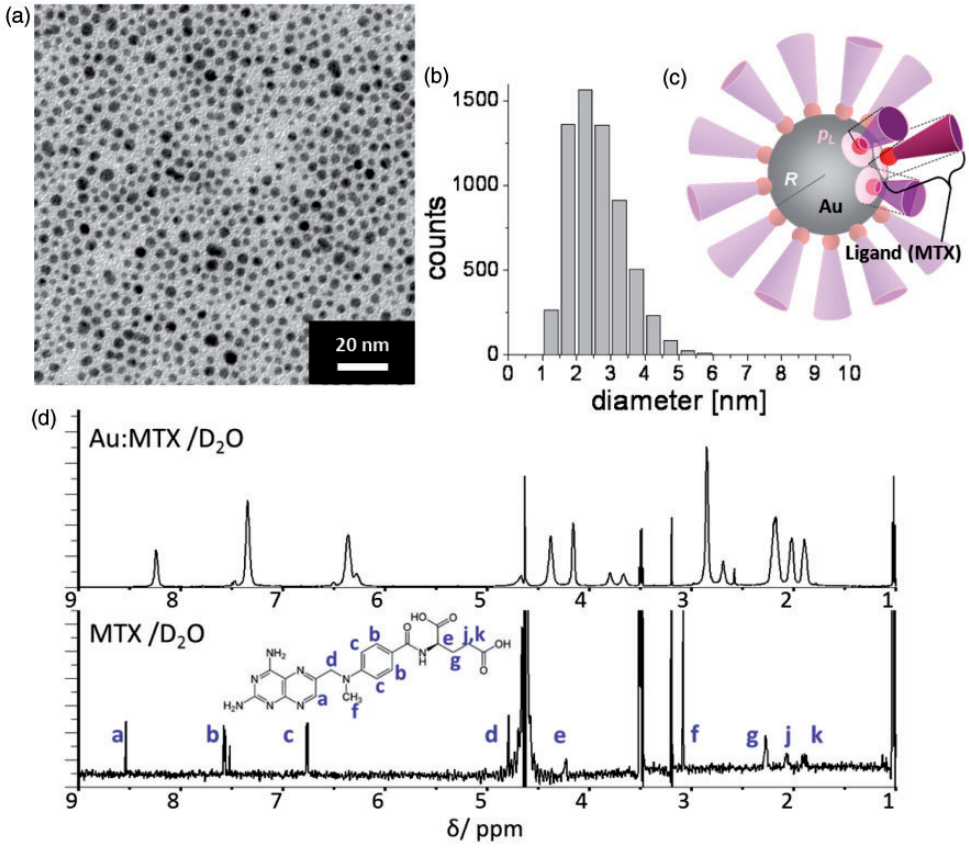


**Figure 1** Methotrexate (MTX)-passivated Au nanoparticles (Au:MTX). (a) Transmission electron microscope (TEM) image of Au:MTX nanoparticles. (b) Size distribution of Au:MTX (2.6 ± 0.7 nm). Histogram was constructed from multiple TEM images. (c) Schematic drawing of drug loading per nanoparticle. *R* is the radius of nanoparticle core, and $p_L$ is the radius of the drug's footprint (or projected area on the nanoparticle core). With Au atomic radius of ~1.44 Å and $2R \sim 2.6$ nm, number of MTX per nanoparticle is ~75, and footprint is ~0.28 nm$^2$ with $2p_L \sim 6$ Å. (d) $^1$H NMR of Au:MTX (top panel) and MTX in $D_2O$ (bottom panel). (A color version of this figure is available in the online journal.)

aromatic ring region of MTX. An aqueous solution of Au:MTX was stable when stored at 4°C, and no significant change was observed over 10 months with TEM and optical spectroscopy (the structural stability of amine-Au nanoparticles in organic phase has been reported by Heath *et al.*[36,37]).

In addition, to demonstrate the wide applicability of the synthesis protocol, we conducted a systematic study on the formation of stable Au nanoparticles using amine-containing molecules with molecular weights (m.w.) ranging from 146.19 (lysine) to 785.55 (flavin adenosine dinucleotide, or FAD), using the same conditions. The results are summarized in Table 1. Despite the relatively weak affinity to Au,[36,37] stable nanoparticles were formed with numerous amine-containing ligands, many of which are drugs in common use. The details of ligand-to-Au interactions require further elucidation. Of particular note, the nanoparticle formation was clearly dependent on the m.w. of the amine ligands: Ligands with m.w. <300 tended to not form colloidally dispersed nanoparticles. The existence of m.w. threshold can be attributed to the effective Au nanoparticle surface coverage for stable colloidal suspension (e.g. reviewed by Templeton *et al.*[26]), and the value of the threshold contrasts with the synthesis of thiol-passivated Au nanoparticles, where the threshold is much known to be smaller[26] at m.w. <100, presumably due to strong thiol-Au affinity.

**Table 1** Formation of monolayer-protected Au nanoparticles

| | Amine compound | Molecular weight | Nanoparticle |
|---|---|---|---|
| 1 | Lysine | 146.19 | Did not form |
| 2 | Methionine | 149.21 | Did not form |
| 3 | Dopamine | 153.18 | Did not form |
| 4 | Arginine | 174.2 | Did not form |
| 5 | Deoxycytidine | 227.27 | Did not form |
| 6 | Cytidine | 243.22 | Did not form |
| 7 | Cytarabine (Ara-C) | 243.22 | Did not form |
| 8 | Deoxyadenosine | 251.24 | Did not form |
| 9 | Adenosine | 267.24 | Did not form |
| 10 | Deoxyguanosine | 267.24 | Did not form |
| 11 | Guanosine | 283.24 | 2.7 ± 1.6 nm |
| 12 | Thiamine | 300.81 | Did not form |
| 13 | Cytidine monophosphate | 323.2 | 4.5 ± 2.8 nm |
| 14 | Adenosine monophosphate | 347.22 | Did not form |
| 15 | Guanosine monophosphate | 363.22 | 2.6 ± 1.0 nm |
| 16 | Cytidine diphosphate | 403.18 | 2.5 ± 0.8 nm |
| 17 | Thyamine pyrophosphate | 425.31 | 3.1 ± 1.3 nm |
| 18 | Adenosine diphosphate | 427.2 | 2.3 ± 0.7 nm |
| 19 | Folic acid | 441.4 | 2.6 ± 1.1 nm |
| 20 | Guanosine diphosphate | 443.2 | 2.4 ± 1.0 nm |
| 21 | Tetracycline | 444.44 | 1.6 ± 0.7 nm |
| 22 | Doxycycline | 444.44 | 1.7 ± 0.7 nm |
| 23 | Methotrexate (MTX) | 454.44 | 2.6 ± 0.7 nm |
| 24 | Methotrexate dimethyl ester | 482.49 | 2.2 ± 0.6 nm |
| 25 | Cytidine triphosphate | 483.16 | 2.6 ± 0.9 nm |
| 26 | Adenosine triphosphate | 507.18 | 2.1 ± 0.7 nm |
| 27 | Guanosine triphosphate | 523.18 | 2.3 ± 0.7 nm |
| 28 | Doxorubicin | 543.52 | 3.3 ± 1.2 nm |
| 29 | Streptomycin | 581.57 | 2.5 ± 1.2 nm |
| 30 | Flavin adenine dinucleotide (FAD) | 785.55 | 4.2 ± 1.6 nm |

Note: Amine-containing compounds are shown in the order according to molecular weight.

## Ligand exchange on Au:MTX and payload release

An important property of Au:MTX is the possibility of controlled MTX release triggered by ligand exchange with thiols. To illustrate this, Au:MTX was mixed and stirred (700 rpm, room temperature) with varied concentrations of glutathione (GSH, Au-to-GSH molar ratio at 0.5, 1, and 5) in water to induce ligand exchange. GSH was chosen as the exchanging thiol because of its ubiquitous endogenous abundance within bio-organisms and its potential relevance to MTX release *in vivo* as well as *in vitro*. MTX-to-GSH ligand exchange was verified: the free MTX in solution at 90 minutes of stirring was measured via UV–vis spectroscopy, and the release of MTX increased according to the GSH concentration (Figure 2(a), also see Supplementary data, Figure S2). Au-to-GSH ratio c.a. >1 saturated the exchange. Also, no significant increase in released MTX was observed after 90 min. Au nanoparticle core size was largely preserved in this ligand exchange (Figure 2(b)), although some degree of aggregation was observed.

## Stability of Au:MTX in physiological conditions

Stability of Au:MTX was examined under physiologically relevant conditions (Figure 3). Au:MTX was surprisingly stable at pH 4–9, and no precipitation or change in the color of solution was observed over 48 h (Figure 3(a)). At pH 2–3, Au:MTX precipitated within 2 h at room temperature. The supernatant of Au:MTX (98 μM in Au molar amounts) precipitated at pH 3 contained ~10 μM MTX that was released as a result of nanoparticle aggregation (Figure 3(b)). It is noted that the gastric environment is at pH ~1.5–3.5, and that the acidity in cell lysosome is at pH ~5. Au:MTX was stable in saline solutions or in the presence of proteins (Figure 3(c)). No precipitation was observed in phosphate buffer saline (PBS), in an albumin solution (bovine serum albumin, or BSA, 35 g/L), or in serum (fetal bovine serum, or FBS, 100%).

## Enhanced efficacy of Au:MTX in vitro

We characterized Au:MTX as drug delivery vehicles and evaluated *in vitro* therapeutic effects. Au:MTX was purified via sets of centrifugal precipitations, and the Au-to-MTX molar ratio (drug loading onto Au nanoparticle) was measured by elemental analyses (carbon–hydrogen–nitrogen analysis (CHN) and inductively coupled plasma mass spectrometry (ICP-MS)). CHN analysis yielded C:N = 1:0.405, in good agreement with MTX chemical formula. Au-to-MTX molar ratio was determined as [Au]:[MTX] = 9.8:1, i.e. one nanoparticle on average carried ~75 MTX molecules (assuming ~1.44 Å as atomic radius of Au and uniform surface coverage, as illustrated in Figure 1(c)).[46] This ratio was

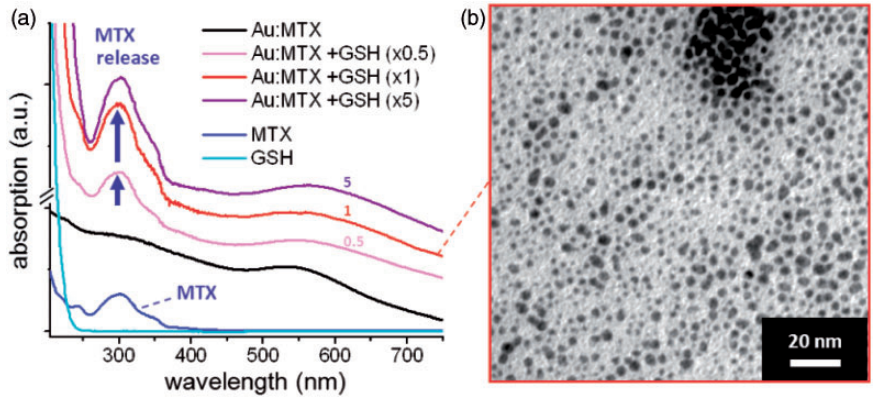


**Figure 2** Controlled payload release from Au:MTX nanoparticles via ligand exchange. (a) Glutathione (GSH)-induced MTX release from Au:MTX characterized using UV–vis absorption spectroscopy. GSH concentration was varied as Au-to-GSH molar ratio =1:0.5 (labeled as ×0.5 in the inset), 1:1 (×1), and 1:5 (×5). (b) TEM image of Au nanoparticles after the ligand exchange (Au-to-GSH molar ratio = 1:1)

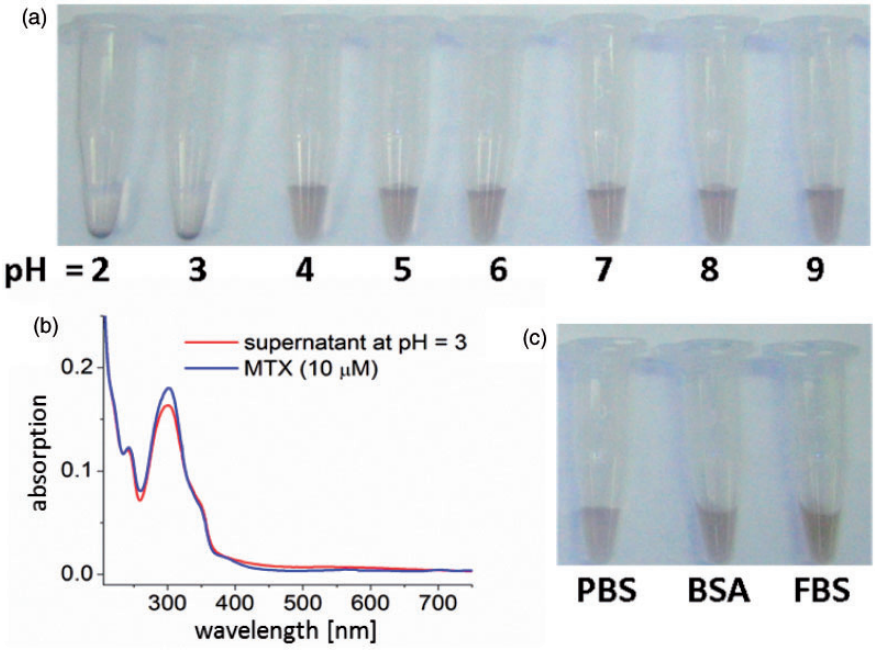


**Figure 3** Stability of Au:MTX under physiologically relevant conditions. (a) Au:MTX nanoparticles are stable at pH 4–9, and precipitates at pH 2–3. (b) Absorption spectrum of the supernatant of precipitated Au:MTX solution (10 μM equimolar in MTX) at pH = 3. MTX molecules are almost fully dissociated from nanoparticles. (c) Au:MTX nanoparticles are stable in saline (PBS) as well as in protein (BSA and FBS) solutions

consistent with the spectroscopic observation in Figure 3(b), when MTX was fully released due to nanoparticle aggregation and precipitation. We used this ratio in the following experiments to determine the MTX drug payload in Au:MTX, such that the net amount of MTX was the same as that of MTX-alone treatment. Drug delivery by Au:MTX was evaluated using a human AML cell line THP-1. THP-1 cells were treated with 50 and 500 nM concentrations (in molar amount of MTX, as determined by the elemental analysis) of Au:MTX, in comparison to treatments with buffer (PBS, as vehicle control), equivalent molar amounts of MTX alone, and folic acid-passivated Au nanoparticles (Au:FOL). Au:FOL, with the diameter $2.6 \pm 1.1$ nm measured by TEM, is structurally similar to Au:MTX (*c.f.* Supplementary data, Figure S3) and was therefore used as an ''Au nanoparticle without active drug'' control. THP-1 growth curves indicate similar efficacy of MTX and Au:MTX treatments at 50 and 500 nM concentrations, thus confirming effective delivery of MTX by nanoparticles (Figure 4(a)). It is important to note that Au:FOL did not exhibit significant effect on cell growth, suggesting very low toxicity caused by Au nanoparticle cores alone. Cellular uptake of Au:MTX was examined *in vitro* (Figure 4(b)). TEM images were taken after THP-1 cells were incubated for 4 hours with 500 nM-MTX equimolar concentration of Au:MTX, and a majority of Au nanoparticles were found dispersed within the cells without forming large-scale aggregations.

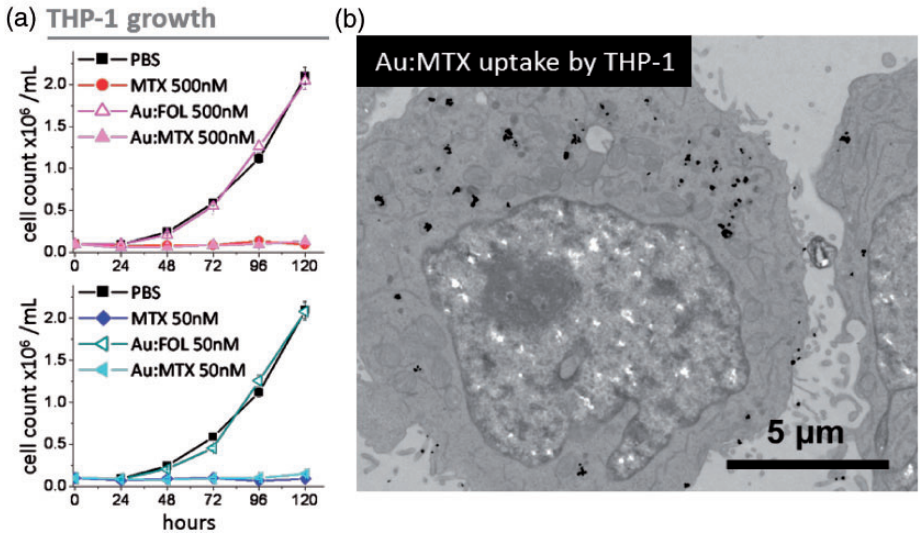


**Figure 4** *In vitro* evaluation of drug delivery by Au:MTX nanoparticles. (a) Growth curves of MTX-, Au:MTX-, and Au:FOL-treated THP-1 (an AML cell line). Cells were treated immediately before the incubation started, with PBS, MTX (500 nM, top panel; 50 nM, bottom panel), as well as equimolar Au:MTX and Au:FOL, so that the MTX payload is equivalent to the MTX-only treatment. Au:FOL does not significantly affect the growth of THP-1. (b) Au:MTX uptake by THP-1 cells examined by TEM. Locations of Au nanoparticles are visualized as black dots in the images, using silver-enhancement technique. (A color version of this figure is available in the online journal.)

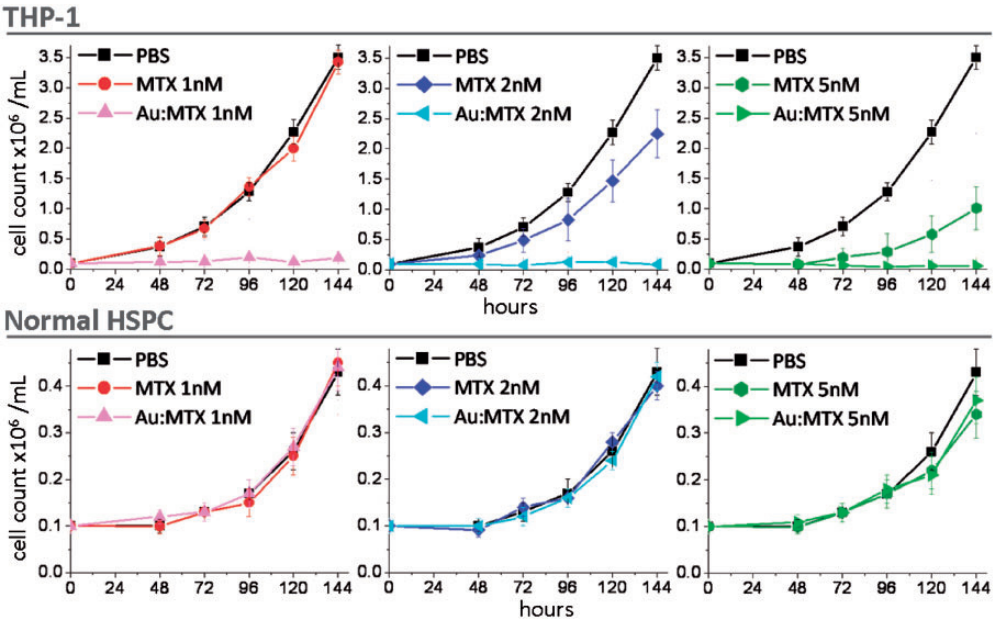


**Figure 5** Au:MTX demonstrating enhanced therapeutic index compared to MTX-alone *in vitro*. Growth curves of MTX- and Au:MTX-treated (1 nM, left panel; 2 nM middle panel; 5 nM, right panel) cancer cells (THP-1, top panels) and normal hematopoietic stem/progenitor cells (HSPCs, bottom panels) are shown. Au:MTX completely inhibits THP-1 growth at 1–5 nM, whereas MTX-alone show dose-dependent THP-1 growth suppression. Moreover, both Au:MTX and MTX-alone do not significantly affect normal HSPC growth at 1–5 nM. (A color version of this figure is available in the online journal.)

Enhanced efficacy of Au:MTX was validated *in vitro* using a human AML cell line THP-1 and normal hematopoietic stem/progenitor cells (HSPCs), as an appropriate normal counterpart to the myeloid cancer cells. THP-1 and HSPCs were treated with 1, 2, and 5 nM concentrations of Au:MTX and MTX (Figure 5). Au:MTX exhibited elevated potency, and therefore enhanced drug delivery, compared to MTX-alone. Au:MTX completely inhibited THP-1 cell growth at 1–5 nM, whereas MTX-alone treatments resulted in dose-dependent suppression. On the other hand, HSPC growth was not significantly affected either by Au:MTX and MTX treatments within the same 1–5 nM dose range. Thus, in comparison to MTX-alone, Au:MTX can produce more selective growth inhibition of cancer (THP-1) cells while sparing normal HSPCs *in vitro*.

### Efficacy and safety of Au:MTX nanoparticles in vivo

In order to evaluate the therapeutic index of Au:MTX *in vivo*, efficacy as well as safety were assessed in a

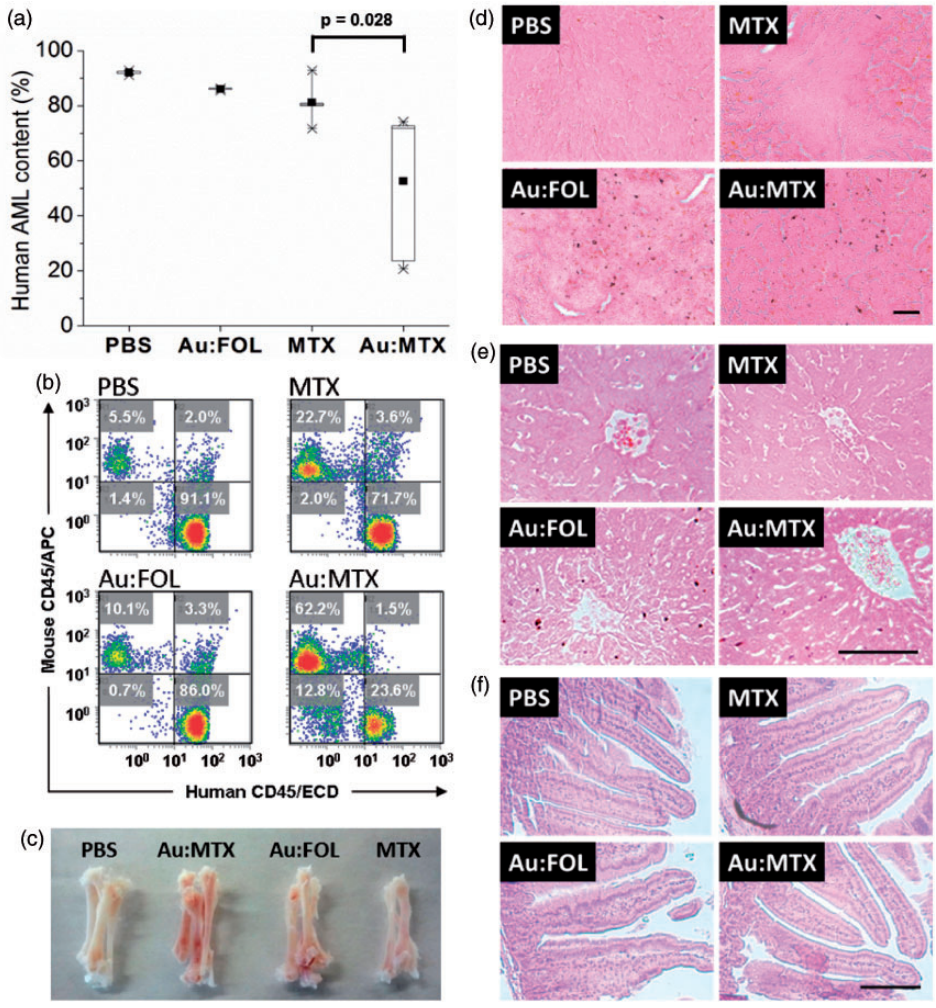


**Figure 6** Au:MTX treatment in a murine xenotransplant model of primary human AML. Therapeutic index of Au:MTX is compared to PBS, MTX, and Au:FOL *in vivo*. (a) Human AML content in bone marrow measured by flow cytometry. Au:MTX-treated group exhibit markedly improved efficacy. (b) Representative raw flow cytometry data. (c) Murine bones before marrow extraction. Murine bones from Au:MTX-treated group exhibit marked suppression of anemia (more red marrow) compared to other three treatment groups. (d) Au nanoparticle delivery *in vivo* is demonstrated in spleens and (e) in livers harvested post-treatment with silver enhancement, and eosin staining. Brown dots in the spleen and liver tissues are the locations of Au nanoparticles visualized via silver-enhancement. (f) Histology of intestines indicate no added damage to endothelium caused by Au:MTX. Scale bars indicate 100 μm in (d) to (f)

murine xenotransplant model of primary human AML (using AML cells obtained from a patient).[47] This model is a relatively faithful representation of the actual human disease, with diffuse infiltration of the bone marrow by human leukemia cells, splenomegaly, and fatality from cytopenia. Au:MTX treatment was compared to PBS, MTX alone, and Au:FOL treatments, all administered intravenously (i.v.) 2×/week by tail vein injection. Based on the literature,[48] we chose the dose of 0.25 mg/kg MTX, and accordingly the dose of Au:MTX and Au:FOL calculated from the drug loading (drug-to-Au molar ratio determined by the elemental analyses). Mice were monitored daily and euthanized at week 6 when the PBS control group demonstrated distress from anemia. Amongst these treatment groups, Au:MTX-treated mice exhibited the least sign of anemia (Supplementary data, Figure S4), the consistently lower bone marrow leukemia cell burden compared to other treatment groups as quantified by flow-cytometry (Figure 6(a) to (c), and Supplementary data, Figure S5), and the lowest splenic leukemia cell burden quantified by weight and histological examination (Figure 6(d) and Supplementary data, Figure S6). There was no evidence of increased toxicity from Au:MTX compared to the other treatments based on the weight, appearance, and behavior of the mice, or in histological examination of the liver and the rapidly proliferating cells, e.g. intestinal endothelium (Figure 6(e) and (f)). Thus, Au:MTX treatment can induce a superior therapeutic index compared to MTX alone or the other treatment arms.

## Discussion

Enhanced therapeutic index of Au:MTX in our primary AML model is a result of the effective delivery of MTX to AML cells compared to normal cells. The detailed mechanistic elucidation of the observed cancer selectivity necessitates further investigation. One contribution could originate from the difference in the rate of uptake among cell types, or the difference between folate receptor-mediated MTX

transport and endocytotic uptake of Au:MTX.[49,50] Another contribution could be the consequence of glutathione-mediated *in situ* ligand exchange of Au:MTX, and the elevated level of glutathione in AML cells resulting in facilitated MTX release. As we demonstrated, release of MTX can be triggered by glutathione. It is known that cancer cells/tissues ubiquitously express higher glutathione levels compared to normal cells/tissues (reviewed by Balendiran *et al.*[51]). High glutathione expressions in AML cell line THP-1 and primary AML cells were confirmed by measuring intracellular glutathione concentrations using an enzymatic recycling assay[52] compared to hematopoietic stem/progenitor cells (HSPCs) from cord blood, a relevant normal cell comparison (Supplementary data, Figure S7).

In summary, we evaluated Au nanoparticles directly passivated with unmodified drugs as a drug delivery platform. Au nanoparticles could be practical drug delivery vehicles, since thorough toxicology studies[53] as well as phase I trials[54] indicate minimal or no toxicity at clinically relevant dosages. Using Au:MTX as an example, we demonstrated the possibility of controlled drug release through competitive affinity between MTX and GSH toward the Au nanoparticle core. Au:MTX exhibited enhanced therapeutic index in the AML models *in vivo* and *in vitro*, possibly through the payload release via ligand exchange, although the detailed mechanism requires further elucidation. The simplicity of the synthesis and composition of these drug-Au nanoparticles facilitates scale-up for clinical evaluation, and versatile application to multitude of therapeutic agents in common use. Controlling nanoparticle size and surface properties would affect the bio-distribution[22,54,55] and may further enhance the therapeutic index. Post-synthesis partial ligand exchange to incorporate additional functional molecules that enhance targeting and/or to confer a tracking modality (e.g. fluorescence) is also feasible and is being evaluated.

**Author contributions:** SE and YS conceived the project and designed the experiments. SE, QE, and YS designed the animal experiments. SE performed nanoparticle syntheses, characterizations, *in vitro* cell experiments, and histology of animal samples. QE performed animal treatments and experiments. RZM performed flow cytometry measurements. SE and YS analyzed the data and wrote the manuscript.

#### ACKNOWLEDGEMENTS

We thank Cleveland Cord Blood Center for providing cord blood samples and K.P. Ng for processing the samples. We also thank M. Yin and D. Mahovlic for their assistance with the biological specimen preparations. This work was supported in part by NIH 1R01CA138858 and U54HL090513, DoD PR081404, and Clinical & Translational Science Collaborative (CTSC) UL1RR024989. SE gratefully acknowledges support from the Lerner Research Institute Chairman's Innovative Research Fund Award and from the Scott Hamilton CARES Initiative Foundation.

#### REFERENCES

1. Strebhardt K, Ullrich A. Paul Ehrlich's magic bullet concept: 100 years of progress. *Nat Rev Cancer* 2008;**8**:473–80
2. Ferrari M. Cancer nanotechnology: opportunities and challenges. *Nat Rev Cancer* 2005;**5**:161–71
3. Alivisatos P. Less is more in medicine. *Sci Am* 2001;**285**:66–73
4. Langer R. Drug delivery and targeting. *Nature* 1998;**392**:5–10
5. Peters D, Kastantin M, Kotamraju VR, Karmali PP, Gujraty K, Tirrell M, Ruoslahti E. Targeting atherosclerosis by using modular, multifunctional micelles. *Proc Natl Acad Sci* 2009;**106**:9815–9
6. Torchilin VP. Recent advances with liposomes as pharmaceutical carriers. *Nat Rev Drug Discov* 2005;**4**:145–60
7. Gregoriadis G, Wills EJ, Swain CP, Tavill AS. Drug-carrier potential of liposomes in cancer chemotherapy. *Lancet* 1974;**1**:1313–6
8. Nance EA, Woodworth GF, Sailor KA, Shih TY, Xu QG, Swaminathan G, Xiang D, Eberhart C, Hanes J. A dense poly(ethylene glycol) coating improves penetration of large polymeric nanoparticles within brain tissue. *Sci Transl Med* 2012;**4**:149ra19
9. Mitragotri S, Lahann J. Materials for drug delivery: innovative solutions to address complex biological hurdles. *Adv Mater* 2012;**24**:3717–23
10. Perry JL, Herlihy KP, Napier ME, DeSimone JM. PRINT: a novel platform toward shape and size specific nanoparticle theranostics. *Acc Chem Res* 2011;**44**:990–8
11. Kabanov AV, Vinogradov SV. Nanogels as pharmaceutical carriers: finite networks of infinite capabilities. *Angew Chem Int Ed Engl* 2009;**48**:5418–29
12. Crampton HL, Simanek EE. Dendrimers as drug delivery vehicles: non-covalent interactions of bioactive compounds with dendrimers. *Polym Int* 2007;**56**:489–96
13. Senter PD. Potent antibody drug conjugates for cancer therapy. *Curr Opin Chem Biol* 2009;**13**:235–44
14. Teicher BA. Antibody-drug conjugate targets. *Curr Cancer Drug Target* 2009;**9**:982–1004
15. Carter P. Improving the efficacy of antibody-based cancer therapies. *Nat Rev Cancer* 2001;**1**:118–29
16. Rana S, Bajaj A, Mout R, Rotello VM. Monolayer coated gold nanoparticles for delivery applications. *Adv Drug Deliv Rev* 2012;**64**:200–16
17. Akhter S, Ahmad MZ, Ahmad FJ, Storm G, Kok RJ. Gold nanoparticles in theranostic oncology: current state-of-the-art. *Expert Opin Drug Deliv* 2012;**9**:1225–43
18. Arvizo R, Bhattacharya R, Mukherjee P. Gold nanoparticles: opportunities and challenges in nanomedicine. *Expert Opin Drug Deliv* 2010;**7**:753–63
19. Boisselier E, Astruc D. Gold nanoparticles in nanomedicine: preparations, imaging, diagnostics, therapies and toxicity. *Chem Soc Rev* 2009;**38**:1759–82
20. Huang X, Jain PK, El-Sayed IH, El-Sayed MA. Gold nanoparticles: interesting optical properties and recent applications in cancer diagnostics and therapy. *Nanomedicine* 2007;**2**:681–93
21. El-Sayed IH, Huang X, El-Sayed MA. Selective laser photo-thermal therapy of epithelial carcinoma using anti-EGFR antibody conjugated gold nanoparticles. *Cancer Lett* 2006;**239**:129–35
22. Chithrani BD, Ghazani AA, Chan WC. Determining the size and shape dependence of gold nanoparticle uptake into mammalian cells. *Nano Lett* 2006;**6**:662–8
23. Egusa S, Redmond PL, Scherer NF. Thermally-driven nanoparticle array growth from atomic Au precursor solutions. *J Phys Chem C* 2007;**111**:17993–6
24. Feldheim DL, Foss CA. *Metal nanoparticles*. New York: Marcel Dekker, 2002
25. El-Sayed MA. Some interesting properties of metals confined in time and nanometer space of different shapes. *Acc Chem Res* 2001;**34**:257–64
26. Templeton AC, Wuelfing WP, Murray RW. Monolayer-protected cluster molecules. *Acc Chem Res* 2000;**33**:27–36
27. Matsumura Y, Maeda H. A new concept for macromolecular therapeutics in cancer chemotherapy: mechanism of tumoritropic accumulation of proteins and the antitumor agent Smancs. *Cancer Res* 1986;**46**:6387–92

28. Podsialdlo P, Sinani VA, Bahng JH, Kam NWS, Lee J, Kotov NA. Gold nanoparticles enhance the anti-leukemia action of a 6-mercaptopurine chemotherapeutic agent. *Langmuir* 2008;**24**:568–74
29. Ulbrich K, Subr V. Polymeric anticancer drugs with pH-controlled activation. *Adv Drug Deliv Rev* 2004;**56**:1023–50
30. Hostetler MJ, Templeton AC, Murray RW. Dynamics of place-exchange reactions on monolayer-protected gold cluster molecules. *Langmuir* 1999;**15**:3782–9
31. Hong R, Han G, Fernández JM, Kim BJ, Forbes NS, Rotello VM. Glutathione-mediated delivery and release using monolayer protected nanoparticle carriers. *J Am Chem Soc* 2006;**128**:1078–9
32. Harmsen S, Dolman MEM, Nemes Z, Lacombe M, Szokol B, Pato J, Keri G, Orfi L, Storm G, Hennink WE, Kok RJ. Development of a cell-selective and intrinsically active multikinase inhibitor bioconjugate. *Bioconjugate Chem* 2011;**22**:540–5
33. Anderson ME. Glutathione: an overview of biosynthesis and modulation. *Chem Biol Interact* 1998;**111–112**:1–14
34. Woehrle GH, Warner MG, Hutchison JE. Ligand exchange reactions yield subnanometer, thiol-stabilized gold particles with defined optical transitions. *J Phys Chem B* 2002;**106**:9979–81
35. Brown LO, Hutchison JE. Convenient preparaiton of stable, narrow-dispersity, gold nanocrystals by ligand exchange reactions. *J Am Chem Soc* 1997;**119**:12384–5
36. Heath JR, Knobler CM, Leff DV. Pressure/temperature phase diagrams and superlattices of organically functionalized metal nanocrystal monolayers: the influence of particle size, size distribution, and surface passivant. *J Phys Chem B* 1997;**101**:189–97
37. Leff DV, Brandt L, Heath JR. Synthesis and characterization of hydrophobic organically-soluble gold nanocrystals functionalized with primary amines. *Langmuir* 1996;**12**:4723–30
38. Rai A, Prabhune A, Perry CC. Antibiotic mediated synthesis of gold nanoparticles with potent antimicrobial activity and their application in antimicrobial coatings. *J Mater Chem* 2010;**20**:6789–98
39. Porta F, Krpetic Z, Prati L, Gaiassi A, Scarì G. Gold-ligand interaction studies of water-soluble aminoalcohol capped gold nanoparticles by NMR. *Langmuir* 2008;**24**:7061–4
40. Wangoo N, Bhasin KK, Mehta S, Suri CR. Synthesis and capping of water-dispersed gold nanoparticles by an amino acid: bioconjugation and binding studies. *J Colloid Interface Sci* 2008;**323**:247–54
41. Joshi H, Shirude PS, Bansal V, Ganesh KN, Sastry M. Isothermal titration calorimetry studies on the binding of amino acids to gold nanoparticles. *J Phys Chem B* 2004;**108**:11535–40
42. Chen S, Ingram RS, Hostetler MJ, Pietron JJ, Murray RW, Schaaff TG, Khoury JT, Alvarez MM, Whetten RL. Gold nanoelectrodes of varied size: transition to molecule–like charging. *Science* 1998;**280**:2098–101
43. Schaaff TG, Knight G, Shafigullin MN, Borkman RF, Whetten RL. Isolation and selected properties of a 10.4 kDa gold: glutathione cluster compound. *J Phys Chem B* 1998;**102**:10643–6
44. Brust M, Walder M, Bethell D, Schiffrin DJ, Whyman R. Synthesis of thiol-derivatised gold nanoparticles in a two-phase liquid-liquid system. *J Chem Soc, Chem Commun* 1994;801–2
45. Chen YH, Tsai CY, Huang PY, Chang MY, Cheng PC, Chou CH, Chen DH, Wang CR, Shiau AL, Wu CL. Methotrexate conjugated to gold nanoparticles inhibits tumor growth in a syngeneic lung tumor model. *Mol Pharm* 2007;**4**:713–22
46. Green SJ, Stokes JJ, Hostetler MJ, Pietron JJ, Murray RW. Three-dimensional monolayers: Nanometer-sized electrodes of alkanethiolate-stabilized gold cluster molecules. *J Phys Chem B* 1997;**101**:2663–8
47. Ng KP, Ebrahem Q, Negrotto S, Mahfouz RZ, Link KA, Hu Z, Gu X, Advani A, Kalaycio M, Sobecks R, Sekeres M, Copelan E, Radivoyevitch T, Maciejewski J, Mulloy JC, Saunthararajah Y. p53 independent epigenetic-differentiation treatment in xenotransplant models of acute myeloid leukemia. *Leukemia* 2011;**25**:1739–50
48. van de Steeg E, van der Kruijssen CM, Wagenaar E, Burggraaff JE, Mesman E, Kenworthy KE, Schinkel AH. Methotrexate pharmacokinetics in transgenic mice with liver-specific expression of human organic anion-transporting polypeptide 1B1 (SLCO1B1). *Drug Metab Dispos* 2009;**37**:277–81
49. Thomas TP, Huang BH, Choi SK, Silpe JE, Kotlyar A, Desai AM, Zong H, Gam J, Joice M, Baker JR. Polyvalent dendrimer-methotrexate as a folate receptor-targeted cancer therapeutic. *Mol Pharm* 2012;**9**(9): 2669–76
50. Jackman AL, Theti DS, Gibbs DD. Antifolates targeted specifically to the folate receptor. *Adv Drug Deliv Rev* 2004;**56**:1111–25
51. Balendiran GK, Dabur R, Fraser D. The role of glutathione in cancer. *Cell Biochem Funct* 2004;**22**:343–52
52. Tietze F. Enzymic method for quantitative determination of nanogram amounts of total and oxidized glutathione: applications to mammalian blood and other tissues. *Anal Biochem* 1969;**27**:502–22
53. Murphy CJ, Gole AM, Stone JW, Sisco PN, Alkilany AM, Goldsmith EC, Baxter SC. Gold nanoparticles in biology: beyond toxicity to cellular imaging. *Acc Chem Res* 2008;**41**:1721–30
54. Libutti SK, Paciotti GF, Byrnes AA, Alexander HR, Gannon WE, Walker M, Seidel GD, Yuldasheva N, Tamarkin L. Phase I and pharmacokinetic studies of CYT-6091, a novel PEGylated colloidal gold-rhTNF nanomedicine. *Clin Cancer Res* 2010;**16**:6139–49
55. De Jong WH, Hagens WI, Krystek P, Burger MC, Sips AJ, Geertsma RE. Particle size-dependent organ distribution of gold nanoparticles after intravenous administration. *Biomaterials* 2008;**29**:1912–9


*(Received January 17, 2014, Accepted March 27, 2014)*